

Article

Fabrication of Anti-HSV-1 Curcumin Stabilized Nanostructured Proniosomal Gel: Molecular Docking Studies on Thymidine Kinase Proteins

Shady M. Abd El-Halim ^{1,*} , Mohamed A. Mamdouh ¹, Alaadin E. El-Haddad ²  and Sara M. Soliman ¹

¹ Department of Pharmaceutics and Industrial Pharmacy, Faculty of Pharmacy, October 6 University, Giza 12585, Egypt; mohamedmamdouh@o6u.edu.eg (M.A.M.); sara.soliman@o6u.edu.eg (S.M.S.)

² Department of Pharmacognosy, Faculty of Pharmacy, October 6 University, Giza 12585, Egypt; alaa_elhaddad.ph@o6u.edu.eg

* Correspondence: shady_mohammed@o6u.edu.eg; Tel.: +20-111-999-4874

Received: 31 January 2020; Accepted: 14 February 2020; Published: 20 February 2020



Abstract: Curcumin is a dietary compound with accrued evidence of antiviral activity. Poor solubility and permeation renders curcumin a good applicant for incorporation into proniosomes. The intent of this study was to formulate curcumin proniosomal gel for topical application and the evaluation of its in-vitro, ex-vivo activities against Herpes Simplex virus type 1 (HSV-1), as well as molecular docking studies on HSV-1 thymidine kinase proteins. Coacervation phase separation tactic, using 2³ full factorial design, was used in the preparation of different proniosomes. Cytotoxicity of the selected formulae (F4 and F8) was evaluated on the Vero cell line. Optimal formulae (F4 and F8) showed entrapment efficiency of 97.15 ± 2.47% and 95.85 ± 2.9%, vesicle size of 173.7 ± 2.26 nm and 206.15 ± 4.17 nm and percentages curcumin released after 3 h of 51.9 ± 1.4% and 50.5 ± 1.1%, respectively. Ex-vivo permeation studies demonstrated that the optimal formulae markedly improved the dermal curcumin delivery. Curcumin proniosomal gel formulae exhibited 85.4% reduction of HSV-1 replication. The ability of curcumin to interact with the key amino acids in the enzyme binding sites of 1KI7, 1KI4, and 1E2P, as indicated by its docking pattern, rationalized its observed activity. Therefore, curcumin proniosomes could be considered as a successful topical delivery system for the treatment of HSV-1.

Keywords: curcumin proniosomal gel; coacervation phase separation; anti-HSV-1; molecular docking; topical delivery system

1. Introduction

Herpes simplex virus type 1 (HSV-1) is a highly contagious pathogen, which is common and endemic throughout the world. It is estimated to affect 60–95% of the adults worldwide [1]. Its ability to institute latency leads to the chronic nature of herpes infection where symptoms may periodically recur in the form of outbreaks of herpetic sores manifesting as burning, watery blisters in the skin or mucous membranes in the mouth and lips [2]. Local treatment with acyclovir is seemingly regarded as the topical therapy standard [3]. The cornerstone of antiviral therapy has been nucleoside analogues such as acyclovir, which, when phosphorylated by viral thymidine kinase, inhibits the viral DNA polymerase by acting as a chain terminator. Combating viral diseases has always been challenging, due to rapid mutation in viral genetics, resulting in resistance to antiviral drugs. Moreover, with most antivirals, side effects hinder their long-term administration [4].

Over the past couple of decades, there has been a growing fascination with functional foods and their perceived health benefits. Such intrigue is advocated by the fact that such natural supplements

are discerned as being safer and less toxic compared to synthesized drugs [5]. An abundance of phytochemicals has exhibited promising antiviral activities [6]. Besides being generally recognized as safe by the FDA [7], turmeric is widely used as a condiment and as a folk medicine for its anti-inflammatory, antioxidant, antiseptic, and anticancer activities, especially in Asian countries [7,8]. Curcumin is the principal curcuminoid derived from turmeric rhizomes (*Curcuma longa* Linn. Zingiberaceae) [9]. Curcumin has been shown to inhibit hepatitis virus, HSV and human papilloma virus by affecting the virus metabolism via apoptosis and cell signaling [10–12]. In addition, curcumin was reported to deactivate histone acetyltransferase of HSV-1 [13].

Unformulated curcumin is reported to afford protection to mice against HSV-2 and its formulation is expected to boost such activity [14]. However, curcumin is a biopharmaceutical classification system (BCS) class IV drug, suffering poor water solubility as well as low permeation capabilities through epithelial tissues [15–17]. Such poor bioavailability represents a challenge, hindering its clinical application. Its incorporation into a nanovesicular system for topical application is expected to provide a tool for enhancing its therapeutic activity.

The formulation of drugs and natural products in novel nanovesicular systems, has gained increasing attention in drug targeting, release control and permeation/bioavailability enhancement [18–25]. Among the attractive nanovesicular systems are proniosomes, which are the dry powder or gel forms of the vesicular system, niosomes. They offer the advantage of improving the vesicles' physical stability by avoiding storage in aqueous medium while preserving their advantages [17,26]. Nonionic surfactants are commonly used in proniosomes due to their stability, wide compatibility and low toxicity [27] whereas, lecithin acts as a permeation enhancer, besides its role in the reduction of vesicular size and limiting drug leakage [28]. Cholesterol is incorporated to increase the stability of the vesicular membrane, whereas added alcohol increases the skin permeability [29]. Finally, the water addition leads to swelling of bilayer, producing spherical multilamellar vesicles [28]. Upon their in-situ hydration, following topical application to the skin under occlusive condition, proniosomal formulations are converted into niosomes that are able to penetrate through the skin [28].

The purpose of this study was to investigate the in-vitro antiviral activity of proniosomal gel containing curcumin on the replication of HSV-1, as well as its ex-vivo activity supported by evidence from molecular docking studies on HSV-1 thymidine kinase proteins.

2. Materials and Methods

2.1. Materials

Curcuma longa rhizomes were purchased from a local herbalist, and kindly identified in the Agricultural Research Center, Cairo, Egypt. Brij 93, Acetonitrile (HPLC grade) and Water (HPLC grade) (Sigma-Aldrich, St. Louis, MO, USA), Trifluoroacetic acid (Alfa Aesar, Karlsruhe, Germany), Soya Lecithin (Carlo Erba Reagents, Barcelona, Spain), Cholesterol (Acros Organics, Fair Lawn, NJ, USA), Kolliphor RH40 (Polyoxyl 35 hydrogenated castor oil, BASF, Ludwigshafen, Germany), Carbopol-940 (kindly supplied by Eva Pharma, Giza, Egypt), Dialysis membrane (12000–14000 M.Wt cut off, Sigma-Aldrich). Other chemicals were of analytical grade.

2.2. Experimental Design

2.2.1. Curcumin Isolation

Powdered *Curcuma longa* rhizome (500 g) were extracted with acetone in soxhlet (3 h), filtered and evaporated (Rotavapor® R-300, BÜCHI, Switzerland). The dried acetone extract (12 g) was defatted with petroleum ether (5 × 1 L) and chromatographed over silica gel CC (2 × 50 cm, 120 g) using CH₂Cl₂:CH₃OH as eluents at different ratios in increasing polarity. Similar fractions were pooled after being checked on TLC silica gel 60 F254 plate. Fractions were dissolved in methanol (100 mL), and heated then chloroform was added (20 mL) and kept at 5 °C overnight. Yellow crystals of curcumin

that precipitated were filtered, purified on Sephadex LH-20 (100 g, 5 × 80 cm) using pure methanol and analyzed by co-spotting against standard curcumin [30].

2.2.2. Formulation Study

In the formulation study, 2³ factorial design was employed to study the effect of 3 different formulation independent variables, which were set at two levels each, namely; surfactant Hydrophilic Lipophilic Balance (HLB) (X1, at low level, Brij 93 with HLB = 4 and high level, Kolliphor RH40 with HLB = 14–16), surfactant amount (X2, at low and high levels) and drug loading (X3, at low and high levels) on the mean vesicle size (Y1) and percentage of entrapment efficiency (Y2). All data were analyzed by ANOVA using Design-Expert[®] software (version 7; Stat-Ease, Inc., Minneapolis, MN, USA) where significance level $p < 0.05$.

2.3. Preparation of Curcumin Proniosomes

Proniosomes were formulated by the previously reported coacervation phase separation technique [26,31]. Simply, accurately weighed amounts of curcumin, cholesterol, nonionic surfactants (Brij 93 or Kolliphor RH40) and soya lecithin were taken in glass vial with addition of absolute ethanol (0.125 mL) (Table 1). All the ingredients were mixed well, the vial open end was lined with a lid to forestall the loss of solvent and warmed over a water bath (60–70 °C, 5 min.) until the mixture entirely dissolved. Distilled water (0.08 mL) was added and the mixture was warmed to obtain a clear solution and allowed to cool down.

Table 1. Composition of curcumin proniosomes formulae and their characterization tests.

Code	Composition (mg) *			Mean Zeta Potential (mV)	PDI	Mean Vesicle Size (nm), (Y ₁)	Entrapment Efficiency (%), (Y ₂)
	Drug	Kolliphor RH40	Brij 93				
F1	6	-	180	-56.57 ± 1.29	0.49	171.40 ± 3.96	41.27 ± 3.91
F2	6	180	-	-39.50 ± 2.10	0.32	161.55 ± 1.06	92.75 ± 2.19
F3	6	-	270	-63.27 ± 0.91	0.48	209.30 ± 0.57	64.75 ± 0.07
F4	6	270	-	-35.20 ± 0.52	0.34	173.70 ± 2.26	97.15 ± 2.47
F5	12	-	180	-66.27 ± 0.59	0.41	250.60 ± 1.27	31.55 ± 1.48
F6	12	180	-	-45.90 ± 1.23	0.52	179.30 ± 0.42	89.00 ± 0.57
F7	12	-	270	-56.97 ± 0.40	0.42	218.05 ± 5.66	50.25 ± 1.77
F8	12	270	-	-45.13 ± 1.32	0.59	206.15 ± 4.17	95.85 ± 2.90

* All formulae contain 90 mg Soya Lecithin and 20 mg Cholesterol in addition to 0.125 mL ethanol and 0.08 mL water.

2.4. Evaluation of Curcumin Proniosomes Formulae

2.4.1. Zeta Potential (ζ) Determination

Zeta potential of the prepared formulae was measured by Laser Doppler velocimetry using Malvern Zetasizer (Malvern Instruments, Malvern, UK) at 25 °C with an angle of detection 173° which measures the electrophoretic mobility and surface charge. Aliquots (0.1 mL) of the hydrated niosomes were measured in triplicates [32].

2.4.2. Vesicle Size and Size Distribution

Vesicle size and polydispersity index (PI) were determined by Zetasizer. Accurate weight of curcumin proniosomes was hydrated 100 times with distilled water. The resulted colloid was sonicated (30 min) (USR3, Julabo Labortechnik, Seelbach, West Germany) then analyzed by adding the produced niosomes (1 mL) into a Malvern's disposable vial [33].

2.4.3. Determination of Percentage Entrapment Efficiency (% EE)

The %EE was carried out using the filtration method [34]. Curcumin proniosomes (0.1 g) were hydrated with distilled water (10 mL) and sonicated (30 min.). By filtration, the resulted niosomes were separated from the untrapped drug. The untrapped poorly water-soluble curcumin was retained over the filter paper, while vesicles passed through its pores. The filtrate (1 mL) was sonicated with adequate amount of methanol (10 min.) to form a clear solution. Curcumin concentration was analyzed spectrophotometrically at λ_{\max} of 419 nm [35,36] and the percentage of drug entrapped was calculated using: $\%EE = (A/B) \times 100$, where A and B are the concentration of curcumin in niosomes after and before filtration respectively.

2.4.4. Optimization of Curcumin Proniosomes

The different prepared formulae were optimized by adjusting Design-Expert® response optimizer with the goal of minimizing the response (Y1, vesicle size) and maximizing the response (Y2, entrapment efficiency).

2.4.5. Preparation of Curcumin Proniosomal Gel

The optimal formulae were converted to proniosomal gel by the addition of an equal volume of 1% carbopol-940 to the hot mixture and then allowed to cool down for further characterizations [37].

2.4.6. Characterization of The Optimal Curcumin Proniosomal Gel Formulae

In-Vitro Release Study

Dialysis membrane was soaked (24 h) in phosphate buffer (pH 7.4). An accurately weighed quantity of proniosomal gel (Formulae F4 and F8), equivalent to 10 mg of curcumin was placed in a glass cylinder (10 × 2.5 cm, 4.91 cm² area), fitted with the presoaked membrane [38,39]. It was then placed in the USP Dissolution Tester vessel (Apparatus I, PTW, Pharma Test, Germany) containing ethanol phosphate buffer (pH 7.4, 250 mL, 32.0 ± 0.5 °C) with continuous stirring (50 rpm). At different time intervals, samples were withdrawn and replaced with ethanol phosphate buffer. The content of curcumin released was analyzed spectrophotometrically at λ_{\max} 419 nm [36].

Ex-Vivo Permeation Studies

The dorsal skin of newly born rats weighing 70 ± 20 g was excised after being sacrificed. The dermal surface was carefully cleaned to remove subcutaneous tissues and adhering fats without damaging the epidermal surface [40].

Permeation of curcumin, through excised rat skin, from the optimal formulae and drug suspension was assessed. The skin was mounted on a diffusion cell such that the stratum corneum was facing the donor compartment. The membrane surface area available for diffusion was 1.7 cm². Proniosomal gel of the optimal formulae equivalent to 10 mg of curcumin was spread evenly on the donor side while the receptor compartment was filled with 14 mL of ethanol phosphate buffer (pH 7.4) at 32.0 ± 0.5 °C and stirred at 50 rpm. At various time intervals, samples from the receptor fluid were withdrawn and replaced with fresh ethanol phosphate buffer. The withdrawn samples were analyzed using HPLC (type LC-20AD, Shimadzu, Japan) comprised of dual pumps (LC-10ADvp), degassing unit (DGU-20A), auto-sampler (SIL-20A) and an UV-vis detector (SPD-20A). Pronto SIL® RP-C18 column (150 × 4.6 mm, 5 µm SC-150, Bischoff Chromatography, Leonberg, Germany) was used in the achievement of the chromatographic separation of curcumin. Data processing and acquisition were conducted utilizing LC solution software (version 1.25 SP4, Shimadzu, Japan). The detector was set at 420 nm. The mobile phase consists of an isocratic mixture of acetonitrile and 0.1% trifluoro-acetic acid (50/50, v/v) with flow rate of 1.5 mL/min. The retention time was 8.6 min for curcumin [41].

The drug flux (permeation rate) at steady state (J_{SS}) was calculated from the slope of linear plot between cumulative amount permeated and time [42]. The permeability coefficient (K_P) was computed using the following equation:

$$K_P = J_{SS}/C_o \quad (1)$$

where, C_o is the initial concentration of the drug ($\mu\text{g/mL}$). Enhancement ratio (E_r) was obtained by dividing J_{SS} of the optimal formulae by J_{SS} of the curcumin suspension [43]: $E_r = J_{SS}$ of formula/ J_{SS} of control.

In-Vitro Anti HSV-1 Assay

Vero Cells.

Vero cells were grown in Eagle's minimum essential medium supplemented with nonessential amino acids (0.5%), L-glutamine (0.2 mM/mL), 10% of newborn calf serum, gentamicin (80 mg/mL), and penicillin (160 U/mL). A virus stock of HSV-1 strain was prepared and the supernatants were stored ($-70\text{ }^\circ\text{C}$) until used [44]. The HSV-1 titer was 2.0×10^6 TCID₅₀/mL (from cytopathogenicity as 50 % tissue culture infectious dose/mL (TCID₅₀/mL).

Cytotoxicity Study (Cell Morphology Evaluation and Cell Viability Assay).

Cytotoxicity study was evaluated microscopically by detecting morphological alterations of Vero cells using inverted light microscope [45]. Cell viability assay was carried out using trypan blue dye exclusion method [46].

Determination of HSV-1 Titers Using Plaque Assay.

Non-toxic dilutions (100 μL) were mixed with 100 μL of HSV-1 doses (1×10^5 , 1×10^6 , 1×10^7). The mixture was incubated ($37\text{ }^\circ\text{C}$, 30 min.). The inoculation of 10-fold dilutions of HSV-1 was carried out into Vero cell line. After the appropriate incubation period, the number of plaques counted after fixation of the cells by formalin and stained with crystal violet (0.4%). The viral titers were expressed as plaque-forming units per milliliter (pfu/mL) [47,48]. Statistical analysis concerning the mean percentage of reduction of HSV-1 replication was carried out using SPSS (version 14.0).

Transmission Electron Microscopy (TEM)

The morphology of F4 proniosomal gel was analyzed by TEM (JEOL, JEM-1230, Tokyo, Japan). After the hydration of proniosomal gel, one drop of the vesicular dispersion was placed as thin film on a carbon-coated copper grid. After that, it was stained with phosphotungstic acid (2%), allowed to dry and remove any excess fluid [49].

Molecular Docking and Targets Preparation

Triangle Matcher placement method and London dG scoring function and MMFF94 force field were used for the docking protocol on Molecular Operating Environment (MOE 2014.0901) software. The X-ray crystallographic structures of thymidine kinase of HSV-I (PDB ID: 1KI7, 1KI4, 1KIM, 1E2P) [50,51] were downloaded from the protein data bank (RCSB PDB, <https://www.rcsb.org>). The proteins and curcumin were protonated, and energy minimized. All minimizations were performed until lowest RMSD gradient ($<2\text{ Kcal. mol}^{-1}\text{ \AA}^{-1}$). Redocking of the co-crystallized ligands (Table S1), was used to validate the docking setup. Curcumin was docked on the validated targets.

3. Results

Proniosomes were prepared utilizing the reported coacervation phase separation technique [26,31]. The effect of 3 different formulation variables was studied using a 2^3 full factorial design, and the effect of surfactant HLB, surfactant amount and drug loading on the mean vesicle size and percentage of entrapment efficiency was statistically analyzed.

3.1. Zeta Potential (ζ), Vesicle Size (VS) and Size Distribution

All formulations were found to be negatively charged with zeta potential values extending from -35.20 ± 0.52 mV to -66.27 ± 0.59 mV, which was expected due to the presence of soya lecithin negative charge. The high values of zeta potential should increase the stability of vesicles by increasing repulsion and preventing their aggregation [52,53]. The mean vesicle size of diluted proniosomes ranged from 161.55 ± 1.06 nm to 250.60 ± 1.27 nm with a low polydispersity index (Table 1). The smaller vesicle size would allow for lowered skin irritation and enhanced skin penetration [34].

ANOVA analysis revealed that all independent variables significantly affected the vesicles size ($p < 0.05$). The 3D response surface plots and the quantitative linear relationship between resultant vesicle size responses with that of the predicted value of all dependent variables are illustrated in Figure 1. The following equation represents the linear regression models for the vesicle size (VS) obtained from the factorial study:

$$VS = 197.02 - 14.34(X_1) + 6.31(X_2) + 15.53(X_3) + 5.94(X_1X_2) - 5.48(X_1X_3) - 8.71(X_2X_3) + 9.88(X_1X_2X_3) \quad (2)$$

where $F = 20.87$, $p < 0.0002$, and adjusted $R^2 = 0.9027$.

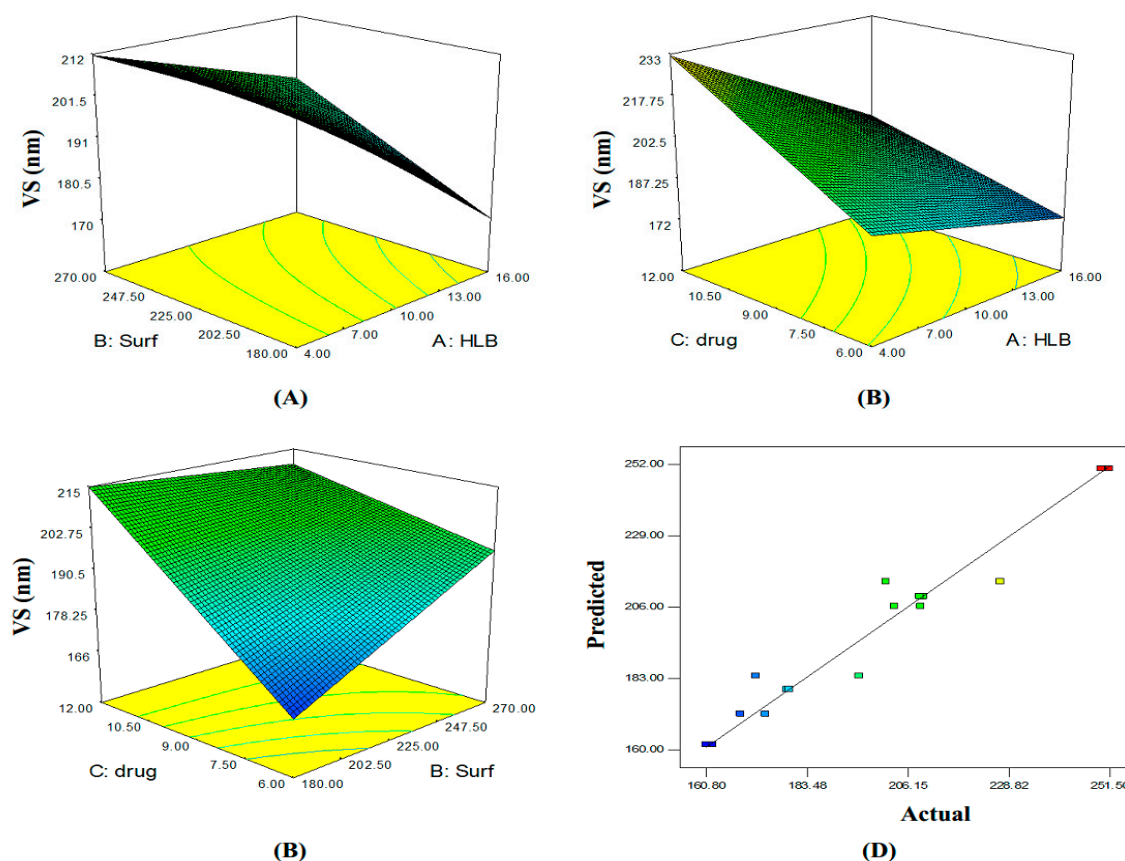


Figure 1. Three-dimensional (A–C) plot and linear correlation plot between actual and predicted values (D) showing the influence of independent variables on the mean vesicle size of curcumin proniosomes formulae (Y1).

3.2. Determination of Percentage Entrapment Efficiency (%EE)

The percentage of curcumin entrapped in the different formulae varied from $31.55 \pm 1.48\%$ to $97.15 \pm 2.47\%$ (Table 1). %EE exhibited a direct positive relationship with HLB value and surfactant concentration, whereas, the opposite was observed for drug loading according to the following equation:

$$\%EE = 70.32 + 23.37(X_1) + 6.68(X_2) - 3.66(X_3) - 3.87(X_1X_2) + 2.40(X_1X_3) - 0.29(X_2X_3) + 0.91(X_1X_2X_3) \quad (3)$$

where $F = 283.83$, $p < 0.0001$, and adjusted $R^2 = 0.9925$.

The 3D response surface plots and the quantitative linear relationship between results of the %EE response with that of the predicted value for all dependent variables are shown in Figure 2.

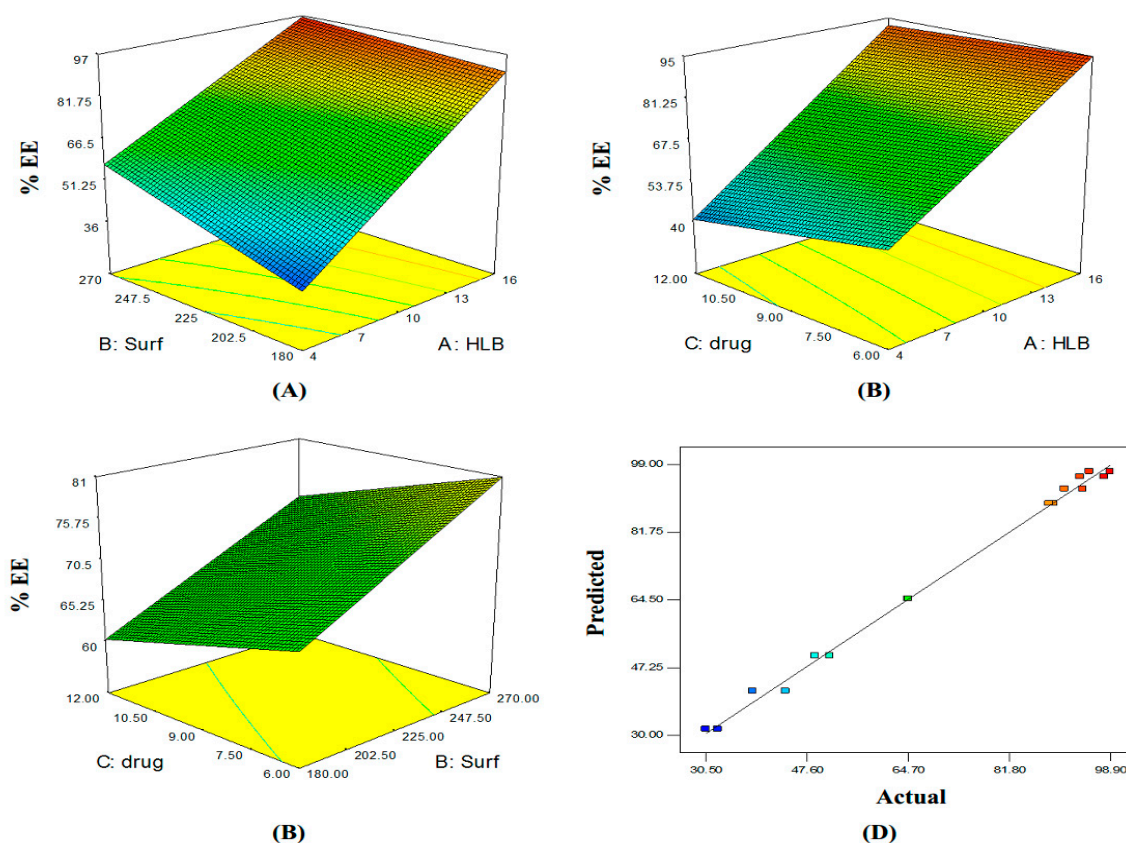


Figure 2. Three-dimensional (A–C) plot and linear correlation plot between actual and predicted values (D) showing the influence of independent variables on the entrapment efficiency of curcumin proniosomes formulae (Y2).

3.3. Optimization of Curcumin Proniosomes

Dosage form optimization was aimed towards determining the levels of independent variables to attain a product with a desirable set of attributes [54]. Formulae prepared with Kolliphor RH40 had smaller vesicle size and higher %EE compared to those prepared using Brij 93. Therefore, formula F4, prepared using Kolliphor with 6 mg drug loading, was selected as the optimized formula by the Design-Expert® software with a desirability value of 0.974.

In addition, F8, with 12 mg drug loading and a desirability value of 0.955, was also selected for further study to evaluate which dose of curcumin is more effective against HSV-1. The two selected formulae (F4 and F8) were converted to proniosomal gel using carbopol 940 (1% w/w).

3.4. Characterization of the Selected Curcumin Proniosomal Gel Formulae

3.4.1. In-Vitro Release Study

The percentage of curcumin that was released from F4 and F8 through a semi-permeable dialysis membrane after 3 h were $51.9 \pm 1.4 \%$ and $50.5 \pm 1.1 \%$, respectively (Figure 3).

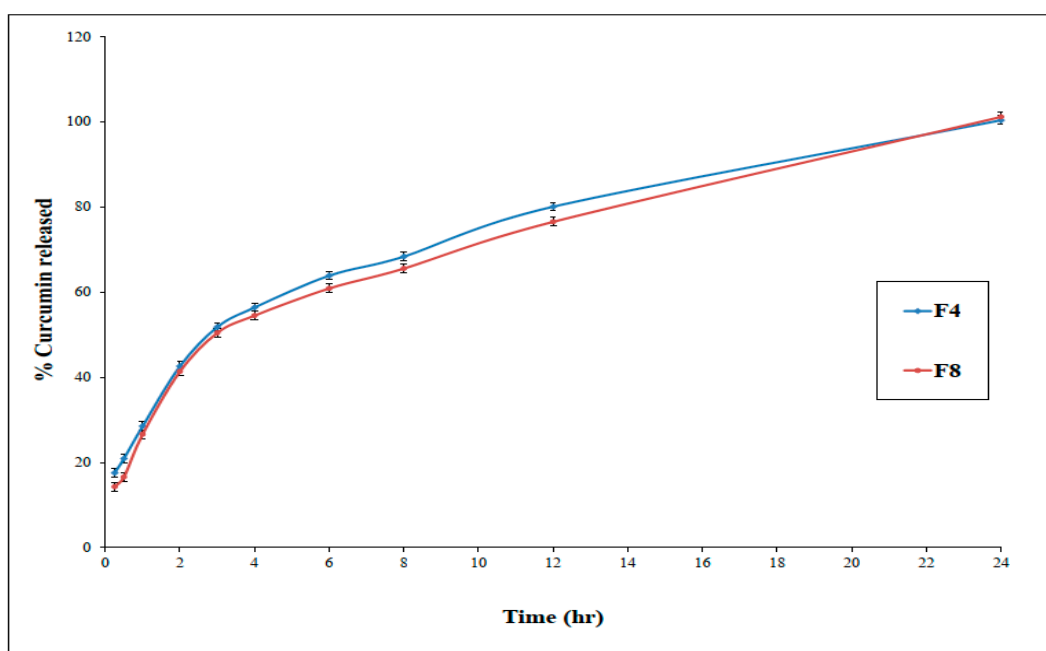


Figure 3. In-vitro release of curcumin from optimized proniosomal gel formulations F4 and F8 (\pm SD, $n = 3$).

3.4.2. Ex-Vivo Permeation Studies

It is difficult to fabricate a simple formulation that enables drug release into the skin. So, the ex-vivo skin permeation test was performed to give great insight into the in-vivo behavior of a newly developed dermal drug delivery system. Based on the observed permeation profiles of curcumin (Figure 4) as well as the different calculated parameters (Table 2), it could be concluded that the loading of curcumin into proniosomes resulted in a significant improvement ($p < 0.05$) in the dermal drug delivery relative to the drug suspension.

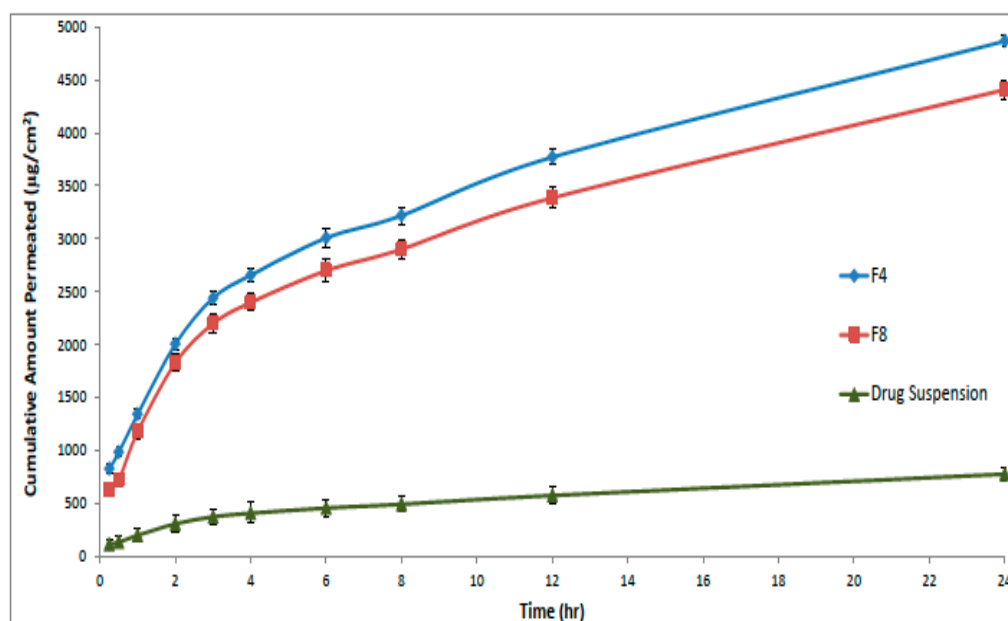


Figure 4. Amount of curcumin permeated at different time intervals across the rat skin membrane from optimal formulae (F4 and F8) compared to the drug suspension (\pm SD, $n = 3$).

Table 2. Permeation data parameters.

Code	Flux (J_{ss}) ($\mu\text{g}/\text{cm}^2/\text{h}$)	K_p (cm/h)	E_r
F4	160.43	0.225	6.14
F8	148.66	0.208	5.69
Drug suspension	26.12	0.037	-

* J_{ss} means permeation rate at steady state; K_p , permeability coefficient and E_r , enhancement ratio.

3.4.3. Cytotoxicity Study of Curcumin on Vero Cells

Assessing the cytotoxicity of an antiviral is crucial when evaluating a potential chemotherapeutic agent, as it shouldn't manifest acute or long-term host toxicity. The effect of pretreatment of Vero cells with curcumin proniosomal gel optimal formulae, (F4 and F8), on HSV-1 replication is shown in Table 3. Statistical analysis confirmed a non-significant difference ($p = 0.33$) between formulae F4 and F8 concerning the mean percentage of the reduction of HSV-1 replication.

However, formulations F4 and F8 significantly ($p < 0.05$) reduced the HSV-1 replication compared to curcumin suspension. Since there is no significant difference between formulae F4 and F8, formula F4, with the lower drug loading, was selected for TEM analysis.

Table 3. The effect of pretreatment of Vero cells with curcumin proniosomal gel formulae on HSV-1 replication.

Tested Materials	Non-Toxic Dose on Vero Cell	Initial Viral Titre	Final Viral Titre	Mean % of Reduction
curcumin suspension	1/100	1×10^5	4×10^4	50 ± 2.2
		1×10^6	4×10^5	
		1×10^7	4×10^6	
F4 (1%)	1/70	1×10^5	5×10^4	85.4 ± 1.05
		1×10^6	5×10^5	
		1×10^7	5×10^6	
F8 (2%)	1/80	1×10^5	5×10^5	87.9 ± 1.65
		1×10^6	4×10^6	
		1×10^7	4×10^7	
Control	1/50	1×10^5	1×10^5	0
		1×10^6	1×10^6	
		1×10^7	1×10^7	

3.4.4. Transmission Electron Microscopy

Hydrated proniosomes photomicrograph of F4 showed spherical niosomal vesicles with well-defined boundaries (Figure 5).

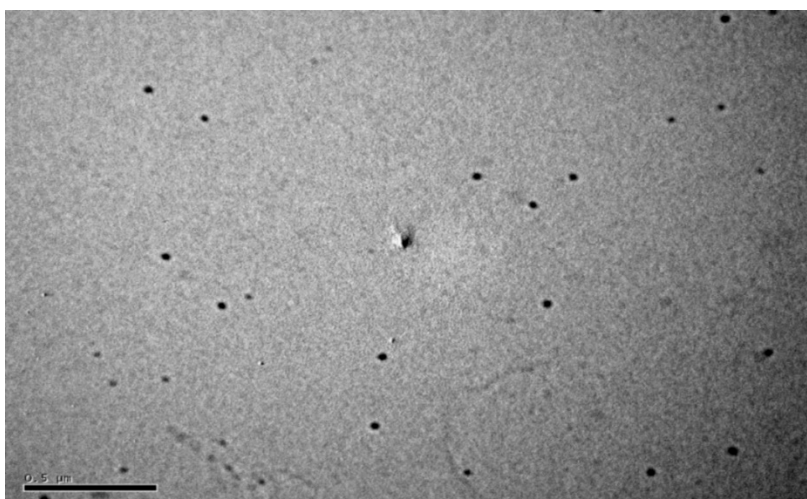


Figure 5. Transmission electron micrograph of niosomes formed after hydration of F4 formula.

3.4.5. Molecular Docking of Curcumin on HSV-1 Thymidine Kinase Proteins

Docking studies of curcumin were performed using MOE software. Redocking of the co-crystallized ligands; 5-Iododeoxyuridine, 5-Bromothienyldeoxyuridine, 6-(dihydroxy-isobutyl)-thymine and Deoxythymidine with enzymes targets; 1KI7, 1KI4, 1E2P and 1KIM respectively, were performed (Figure S1). The validated setup was used in predicting the curcumin-receptor interactions. In 1KI7, the binding pocket is mainly composed of conserved Glu 225, Glu 83, Gln 125, Tyr 101, Arg 163 and Tyr 172. The main key interactions include H-bonds and pi-pi interaction between amino acid residues and ligand. Curcumin interacts by H-bond between the carbonyl group and Tyr 101 side chain; moreover, it also interacts via 2 H-bonds with the Glu 225 side chain (Table 4 and Figure 6).

Table 4. Docked conformations of curcumin with HSV-1 thymidine kinase proteins.

HSV-1 Thymidine Kinase Proteins	Energy Score (kcal/mol)	No. of Interactions	H Bonding Residues	Distance/E (kcal/mol)
1KI7	−5.4	3	GLU 225	3.44/−0.7
			GLU 225	3.34/−0.8
			TYR 101	2.94/−0.9
1KI4	−3.8	6	GLN 125	3.14/−1.1
			MET 128	2.91/−1.8
			GLU 83	2.48/−1.3
			HOH 568	2.45/1.3
			HOH 572	2.65/−1.0
			GLN 125	2.86/−1.6
1E2P	−7.318	4	ARG 163 (pi-H)	3.51/−0.6
			GLN 125	2.73/−2.4
			HOH 2009	2.96/−1.0
			HOH 2036 (pi-H)	4.22/−1.4
1KIM	Not docked	-	-	-

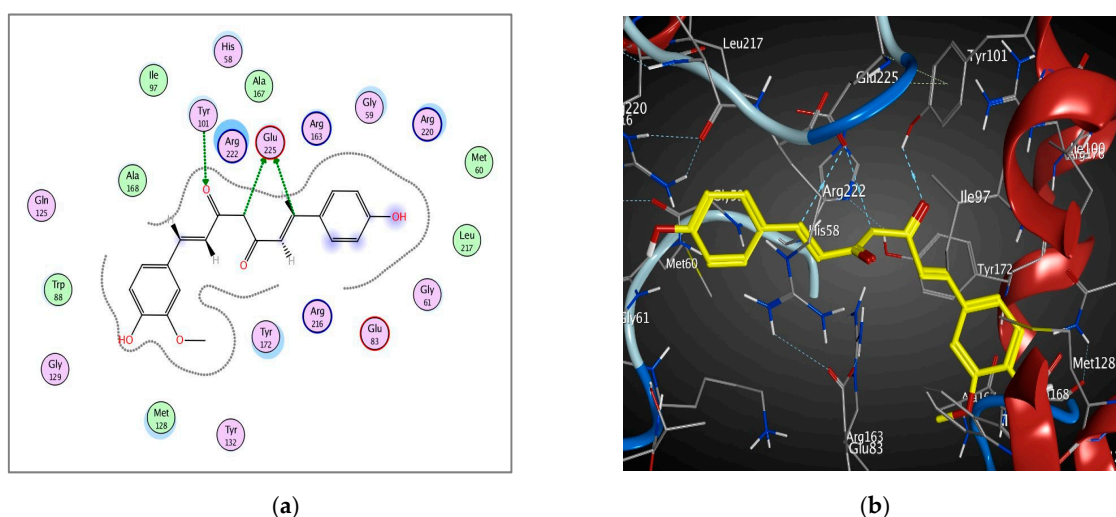


Figure 6. 2D diagram (a) and 3D representation (b) showing the binding mode of curcumin (yellow) with 1KI7 thymidine kinase binding pocket.

The binding pocket of 1KI4 is mainly composed of conserved Glu 225, Glu 83, Gln 125, Tyr 101, Met 128, Arg 176, Arg 163 and Tyr 172. The main key interactions include H-bonds and pi-H interaction between amino acid residues, water molecules and ligand. The 2 carbonyl groups of curcumin interact by 3 H-bonds with the side chains of Arg 176 and Gln 125 amino acids. Curcumin also interacts by H-bond with the side chain of Gln 125 (Table 4 and Figure 7). The 2 phenolic hydroxyl groups interact with Met 128 and Glu 83 by H-bonds. Moreover, Pi-H interaction occurs between aromatic ring of curcumin and Arg 163 residue.

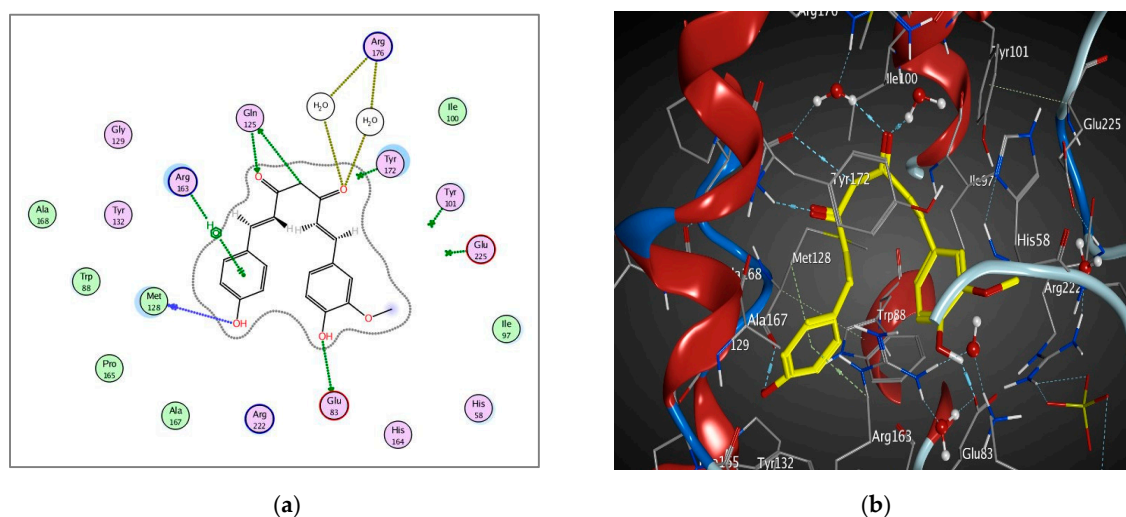


Figure 7. 2D diagram (a) and 3D representation (b) showing the binding mode of curcumin (yellow) with 1KI4 thymidine kinase binding pocket.

The binding pocket of 1E2P is mainly composed of conserved Gln 125, Tyr 172, Glu 83, and Arg 163. The main key interactions include H-bonds, pi-H and pi-pi interactions between amino acid residues, water molecules and ligands. Curcumin interacts through the carbonyl group via the water mediated H-bond with the Tyr 101 amino acid. Curcumin also interacts via the H-bond with Gln 125 amino acid. The phenolic hydroxyl group interacts with Glu 125 via the H-bond. The Pi-H and Pi-Pi interactions were observed between aromatic rings of curcumin and HOH 2036 and Tyr 172 residues, respectively (Table 4 and Figure 8).

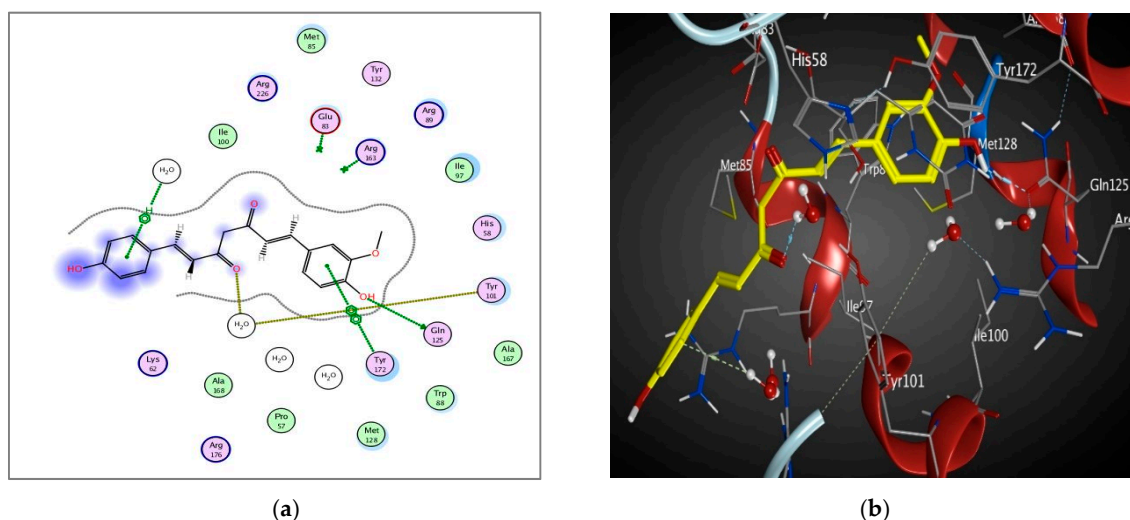


Figure 8. 2D diagram (a) and 3D representation (b) showing the binding mode of curcumin (yellow) with the 1E2P thymidine kinase binding pocket.

4. Discussion

Curcumin was extracted from powdered *Curcuma* rhizomes and purified before being formulated into proniosomes. A 2^3 full factorial design was used to study the effect of three formulation variables, viz; surfactant HLB, surfactant concentration and drug loading on the vesicles size and the percentage of entrapped drug. It was obvious that using a high HLB surfactant (Kolliphor RH40), resulted in the formation of smaller vesicles compared to the low HLB surfactant (Brij 93). These findings were in accordance with Sambhakar et al. [29], where smaller vesicles were obtained upon using tweens rather than spans, which is due to the larger head groups and decreasing length of alkyl chains in the structure of high HLB surfactants [55]. On the other hand, increasing the surfactant concentration led to an increase in the vesicle size. This could be attributed to the more efficient hydration of the uniform thin film at lower surfactant amounts [56] or to the overall increase in hydrophilicity which allows for more water intake into the vesicles core and results in a subsequent increase in size [57]. The observed increase in vesicle size with increasing drug loading might be attributed to the entrapment of the drug in the hydrophobic domain, leading to vesicle size increase [58].

Curcumin entrapment was found to be higher in case of proniosomes prepared with Kolliphor RH40 (high HLB) when compared to Brij 93 (low HLB). These results are in accordance with the findings by Ramezani et al. [59], who reported higher entrapment efficiencies in formulae with higher HLB due to the facilitation of vesicle formation. The increase in surfactant concentration resulted in increased entrapment efficiency. This might be due to the increase in niosomes number; therefore, the volume of hydrophobic bilayer available for housing the hydrophobic drug increases [60]. Meanwhile, the increased drug loading failed to increase the %EE, probably due to a fixed available hydrophobic area for encapsulation at fixed components amounts, with the excess drug being precipitated [61].

The release of curcumin from the optimum formulations was biphasic, with an initial relatively rapid phase followed by a slower permeation phase. The initial rapid phase might be due to the desorption of curcumin from the vesicle surface, while the slower phase was regulated by diffusion through the swollen vesicle bilayers [62]. The initial fast permeation of the drug from the niosomes could help achieve initial epidermis saturation required for successful drug delivery [63].

The observed permeation improvement of curcumin proniosomes could be attributed to the penetration enhancing capabilities of the included surfactants in the fabrication of proniosomes, which are known by their ability to increase fluidity, solubilize, and extract lipid component of the stratum corneum. Keratin interactions are considered as an additional mechanism through which the surfactants can exert penetration enhancing effects [34]. In addition, the formed niosomes also

can enhance the permeability of drugs through structure modification of stratum corneum [64]. Additionally, adsorption and fusion of the formed niosomes onto the surface of skin leads to a high thermodynamic activity gradient of the drug at the interface, which is thought to be the main driving force for the permeation of lipophilic species [42]. This effect is signified by the presence of lecithin which is widely known to impart a high affinity between the vesicle and skin surface layers [65]. Therefore, the optimal proniosomes formulae had successfully enhanced curcumin cutaneous permeation in comparison to curcumin suspension, thus ensuring a promising topical delivery of the drug.

The selected formulations, F4 and F8, exhibited a significant in vitro reduction in the HSV-1 replication compared to the curcumin suspension. The exact interaction of curcumin with the virus was elucidated with the help of molecular docking. Antiherpes therapies principally target thymidine kinases, a key functional protein in DNA synthesis and cell division. Therefore, targeting such protein effectively controls the virus multiplication and the disease. The ability of curcumin to interact with 2, 4, and 3 of amino acids in the binding sites of 1KI7, 1KI4, and 1E2P enzymes respectively, might rationalize its observed activity as indicated by the good docking pattern compared to co-crystallized ligands.

Curcumin bound to the 1E2P protein with the lowest binding energy ($S = -7.318$, 4 interactions) among all the studied proteins. Interactions with 1KI7 protein were assured by S scores = -5.4 and 3 interactions. Antiherpes activity of curcumin will be limited by its low bioavailability and high light instability. Hence, our results can be considered as a primary step in elucidating curcumin antiviral activity and agreed with the previously published work [12,66].

5. Conclusions

The optimal curcumin proniosomal gel formula, composed of high amount of Kolliphor RH40 and low drug loading, showed high entrapment efficiency with optimal mean vesicle size and desirable drug release. There was a significant improvement in the dermal permeation of curcumin, accompanied by 85.4% reduction of HSV-1 replication. The negative binding energy of interaction of curcumin with HSV-1 thymidine kinase proteins *viz.* 1KI7, 1KI4 and 1E2P, justifies the observed activity. These results suggest that proniosomes could be considered as a successful topical antiherpes form of curcumin and could pave the road for clinical studies considering potential of curcumin to treat HSV-1.

Supplementary Materials: The following are available online at <http://www.mdpi.com/2218-0532/88/1/9/s1>.

Author Contributions: Formal analysis: S.M.A.E.-H., M.A.M., A.E.E.-H. and S.M.S. Methodology: S.M.A.E.-H., A.E.E.-H. and S.M.S. Resources: A.E.E.-H. and S.M.S. Writing—original draft: S.M.A.E.-H., A.E.E.-H. and S.M.S. Writing—review & editing: M.A.M. All authors have read and agreed to the published version of the manuscript.

Funding: This research did not receive any specific grant from funding agencies in the public, commercial, or not-for-profit sectors.

Conflicts of Interest: The authors declare no conflict of interest.

References

1. Marchi, S.; Trombetta, C.M.; Gasparini, R.; Temperton, N.; Montomoli, E. Epidemiology of herpes simplex virus type 1 and 2 in Italy: A seroprevalence study from 2000 to 2014. *J. Prev. Med. Hyg.* **2017**, *58*, E27–E33.
2. Cortesi, R.; Ravani, L.; Rinaldi, F.; Marconi, P.; Drechsler, M.; Manservigi, M.; Argnani, R.; Menegatti, E.; Esposito, E.; Manservigi, R. Intranasal immunization in mice with non-ionic surfactants vesicles containing HSV immunogens: A preliminary study as possible vaccine against genital herpes. *Int. J. Pharm.* **2013**, *440*, 229–237. [[CrossRef](#)]
3. Arduino, P.G.; Porter, S.R. Oral and perioral herpes simplex virus type 1 (HSV-1) infection: Review of its management. *Oral Dis.* **2006**, *12*, 254–270. [[CrossRef](#)]
4. Elena, S.F.; Sanjuán, R. Adaptive value of high mutation rates of RNA viruses: Separating causes from consequences. *J. Virol.* **2005**, *79*, 11555–11558. [[CrossRef](#)]
5. Kotha, R.R.; Luthria, D.L. Curcumin: Biological, pharmaceutical, nutraceutical, and analytical aspects. *Molecules* **2019**, *24*, 2930. [[CrossRef](#)]

6. Sanghai, V.D.N.; Kulkarni, S.R.; Sanghai, N.N. Screening of antiviral compounds from plants—A review. *J. Pharm. Res.* **2014**, *8*, 1050–1058.
7. Gupta, S.C.; Patchva, S.; Aggarwal, B.B. Therapeutic roles of curcumin: Lessons learned from clinical trials. *AAPS J.* **2013**, *15*, 195–218. [[CrossRef](#)]
8. Aggarwal, B.B.; Yuan, W.; Li, S.; Gupta, S.C. Curcumin-free turmeric exhibits anti-inflammatory and anticancer activities: Identification of novel components of turmeric. *Mol. Nutr. Food Res.* **2013**, *57*, 1529–1542. [[CrossRef](#)]
9. Flores, D.J.; Lee, L.H.; Adams, S.D. Inhibition of curcumin-treated Herpes Simplex virus 1 and 2 in vero cells. *Adv. Microbiol.* **2016**, *6*, 276–287. [[CrossRef](#)]
10. Qin, Y.; Lin, L.; Chen, Y.; Wu, S.; Si, X.; Wu, H.; Zhai, X.; Wang, Y.; Tong, L.; Pan, B.; et al. Curcumin inhibits the replication of enterovirus 71 in vitro. *Acta Pharm. Sin. B* **2014**, *4*, 284–294. [[CrossRef](#)]
11. Joe, B.; Vijaykumar, M.; Lokesh, B.R. Biological properties of curcumin-cellular and molecular mechanisms of action. *Crit. Rev. Food Sci. Nutr.* **2004**, *44*, 97–111. [[CrossRef](#)] [[PubMed](#)]
12. Mathew, D.; Hsu, W.L. Antiviral potential of curcumin. *J. Funct. Foods* **2018**, *40*, 692–699. [[CrossRef](#)]
13. Kutluay, S.B.; Doroghazi, J.; Roemer, M.E.; Triezenberg, S.J. Curcumin inhibits herpes simplex virus immediate-early gene expression by a mechanism independent of p300/CBP histone acetyltransferase activity. *Virology* **2008**, *373*, 239–247. [[CrossRef](#)]
14. Bourne, K.Z.; Bourne, N.; Reising, S.F.; Stanberry, L.R. Plant products as topical microbicide candidates: Assessment of in vitro and in vivo activity against herpes simplex virus type 2. *Antiviral Res.* **1999**, *42*, 219–226. [[CrossRef](#)]
15. Maiti, K.; Mukherjee, K.; Gantait, A.; Saha, B.P.; Mukherjee, P.K. Curcumin-phospholipid complex: Preparation, therapeutic evaluation and pharmacokinetic study in rats. *Int. J. Pharm.* **2007**, *330*, 155–163. [[CrossRef](#)]
16. Toden, S.; Goel, A. The holy grail of curcumin and its efficacy in various diseases: Is bioavailability truly a big concern? *J. Restor. Med.* **2017**, *6*, 27–36. [[CrossRef](#)]
17. Wahlang, B.; Pawar, Y.B.; Bansal, A.K. Identification of permeability-related hurdles in oral delivery of curcumin using the Caco-2 cell model. *Eur. J. Pharm. Biopharm.* **2011**, *77*, 275–282. [[CrossRef](#)]
18. El-Haddad, A.E.; Sheta, N.M.; Boshra, S.A. Isolation, formulation, and efficacy enhancement of morin emulsified carriers against lung toxicity in rats. *AAPS PharmSciTech* **2018**, *19*, 2346–2357. [[CrossRef](#)]
19. Bayindir, Z.; Yuksel, N. Provesicles as novel drug delivery systems. *Curr. Pharm. Biotechnol.* **2015**, *16*, 344–364. [[CrossRef](#)]
20. Yasam, V.R.; Jakki, S.L.; Natarajan, J.; Kuppusamy, G. A review on novel vesicular drug delivery: Proniosomes. *Drug Deliv.* **2014**, *21*, 243–249. [[CrossRef](#)]
21. Verma, P.; Prajapati, S.K.; Yadav, R.; Senyschyn, D.; Shea, P.R.; Trevaskis, N.L. Single intravenous dose of novel flurbiprofen-loaded proniosome formulations provides prolonged systemic exposure and anti-inflammatory effect. *Mol. Pharm.* **2016**, *13*, 3688–3699. [[CrossRef](#)]
22. Taghipour, Y.D.; Bahramsoltani, R.; Marques, A.M.; Naseri, R.; Rahimi, R.; Haratipour, P.; Panah, A.I.; Farzaei, M.H.; Abdollahi, M. A systematic review of nano formulation of natural products for the treatment of inflammatory bowel disease: Drug delivery and pharmacological targets. *DARU J. Pharm. Sci.* **2018**, *26*, 229–239. [[CrossRef](#)]
23. M Soliman, S.; M Sheta, N.; M.M. Ibrahim, B.; M El-Shawwa, M.; M Abd El-Halim, S. Novel intranasal drug delivery: Geraniol charged polymeric mixed micelles for targeting cerebral insult as a result of ischaemia/reperfusion. *Pharmaceutics* **2020**, *12*, 76. [[CrossRef](#)]
24. Zafar; Quarta; Marradi; Ragusa. Recent developments in the reduction of oxidative stress through antioxidant polymeric formulations. *Pharmaceutics* **2019**, *11*, 505. [[CrossRef](#)]
25. Dei Cas, M.; Ghidoni, R. Dietary Curcumin: Correlation between bioavailability and health potential. *Nutrients* **2019**, *11*, 2147. [[CrossRef](#)]
26. Jadhav, K.R.; Pawar, A.Y.; Bachhav, A.A.; Ahire, S.A. Proniosome: A novel non-ionic provesicles as potential drug carrier. *Asian J. Pharm.* **2016**, *10*, 210–222.
27. Kumar, G.P.; Rajeshwarrao, P. Nonionic surfactant vesicular systems for effective drug delivery—An overview. *Acta Pharm. Sin. B* **2011**, *1*, 208–219. [[CrossRef](#)]
28. Rawat, A.S.; Kumar, M.S.; Khurana, B.; Mahadevan, N. Proniosome gel: A novel topical delivery system. *Int. J. Rec. Adv. Pharm. Res.* **2011**, *3*, 1–10.

29. Sambhakar, S.; Paliwal, S.; Sharma, S.; Singh, B. Formulation of risperidone loaded proniosomes for effective transdermal delivery: An in-vitro and in-vivo study. *Bull. Fac. Pharmacy, Cairo Univ.* **2017**, *55*, 239–247. [[CrossRef](#)]
30. Revathy, S.; Elumalai, S.; Antony, M.B. Isolation, purification and identification of curcuminoids from turmeric (*Curcuma longa* L.) by column chromatography. *J. Exp. Sci.* **2011**, *2*, 21–25.
31. Khatoon, M.; Shah, K.U.; Din, F.U.; Shah, S.U.; Rehman, A.U.; Dilawar, N.; Khan, A.N. Proniosomes derived niosomes: Recent advancements in drug delivery and targeting. *Drug Deliv.* **2017**, *24*, 56–69. [[CrossRef](#)] [[PubMed](#)]
32. Nimbawar, M.; Upadhye, K.; Dixit, G. Fabrication and evaluation of ritonavir proniosomal transdermal gel as a vesicular drug delivery system. *Pharmacophore* **2016**, *7*, 82–95.
33. Loona, S.; Gupta, N.B.; Khan, M.U. Preparation and characterization of metformin proniosomal gel for treatment of diabetes mellitus. *Int. J. Pharm. Sci. Rev. Res.* **2012**, *15*, 108–114.
34. Soliman, S.M.; Abdelmalak, N.S.; El-Gazayerly, O.N.; Abdelaziz, N. Novel non-ionic surfactant proniosomes for transdermal delivery of lacidipine: Optimization using 23factorial design and in vivo evaluation in rabbits. *Drug Deliv.* **2016**, *23*, 1608–1622. [[CrossRef](#)] [[PubMed](#)]
35. Kaur, S.; Kaur, L. Spectrophotometric method for simultaneous estimation of ornidazole and curcumin in pure form. *Pharma Innov.* **2014**, *3*, 1–4.
36. Sharma, K.; Agrawal, S.S.; Gupta, M. Development and validation of UV spectrophotometric method for the estimation of curcumin in bulk drug and pharmaceutical dosage forms. *Int. J. Drug Dev. Res.* **2017**, *4*, 375–380.
37. Lather, V.; Sharma, D.; Pandita, D. Proniosomal gel-mediated transdermal delivery of bromocriptine: In vitro and ex vivo evaluation. *J. Exp. Nanosci.* **2016**, *11*, 1044–1057. [[CrossRef](#)]
38. El-Nabarawi, M.A.; Bendas, E.R.; El Rehem, R.T.A.; Abary, M.Y.S. Transdermal drug delivery of paroxetine through lipid-vesicular formulation to augment its bioavailability. *Int. J. Pharm.* **2013**, *443*, 307–317. [[CrossRef](#)]
39. El-Nabarawi, M.A.; Bendas, E.R.; Abd El Rehem, T.R.; Abary, M.Y.S. Formulation and evaluation of dispersed paroxetine liposomes in gel. *J. Chem. Pharm. Res.* **2012**, *4*, 2209–2222.
40. Abd-Elsalam, W.H.; El-Zahaby, S.A.; Al-Mahallawi, A.M. Formulation and in vivo assessment of terconazole-loaded polymeric mixed micelles enriched with Cremophor EL as dual functioning mediator for augmenting physical stability and skin delivery. *Drug Deliv.* **2018**, *25*, 484–492. [[CrossRef](#)]
41. Jadhav, B.K.; Mahadik, K.R.; Paradkar, A.R. Development and validation of improved reversed phase-HPLC method for simultaneous determination of curcumin, demethoxycurcumin and bis-demethoxycurcumin. *Chromatographia* **2007**, *65*, 483–488. [[CrossRef](#)]
42. Shah, J.; Nair, A.B.; Shah, H.; Jacob, S.; Shehata, T.M.; Morsy, M.A. Enhancement in antinociceptive and anti-inflammatory effects of tramadol by transdermal proniosome gel. *Asian J. Pharm. Sci.* **2019**, *in press*, e1–e11. [[CrossRef](#)]
43. Üstündağ Okur, N.; Apaydin, Ş.; Karabay Yavaşoğlu, N.Ü.; Yavaşoğlu, A.; Karasulu, H.Y. Evaluation of skin permeation and anti-inflammatory and analgesic effects of new naproxen microemulsion formulations. *Int. J. Pharm.* **2011**, *416*, 136–144. [[CrossRef](#)]
44. Amoros, M.; Sauvager, F.; Girre, L.; Cormier, M. In vitro antiviral activity of propolis. *Apidologie* **1992**, *23*, 231–240. [[CrossRef](#)]
45. Simões, C.M.O.; Amoros, M.; Girre, L. Mechanism of antiviral activity of triterpenoid saponins. *Phyther. Res. An Int. J. Devoted to Pharmacol. Toxicol. Eval. Nat. Prod. Deriv.* **1999**, *13*, 323–328. [[CrossRef](#)]
46. Walum, E.; Stenberg, K.; Jenssen, D. Cell toxicology: Principles and practice. *J. Appl. Toxicol.* **1990**, *11*, 389–390.
47. Langlois, M.; Allard, J.P.; Nugier, F.; Aymard, M. A rapid and automated colorimetric assay for evaluating the sensitivity of herpes simplex strains to antiviral drugs. *J. Biol. Stand.* **1986**, *14*, 201–211. [[CrossRef](#)]
48. Kruppenbacher, J.P.; Klass, R.; Eggers, H.J. A rapid and reliable assay for testing acyclovir sensitivity of clinical herpes simplex virus isolates independent of virus dose and reading time. *Antiviral Res.* **1994**, *23*, 11–22. [[CrossRef](#)]
49. Sezgin-Bayindir, Z.; Yuksel, N. Investigation of formulation variables and excipient interaction on the production of niosomes. *AAPS PharmSciTech* **2012**, *13*, 826–835. [[CrossRef](#)]

50. Champness, J.N.; Bennett, M.S.; Wien, F.; Visse, R.; Summers, W.C.; Herdewijn, P.; de Clerq, E.; Ostrowski, T.; Jarvest, R.L.; Sanderson, M.R. Exploring the active site of herpes simplex virus type-1 thymidine kinase by X-ray crystallography of complexes with aciclovir and other ligands. *Proteins* **1998**, *32*, 350–361. [[CrossRef](#)]
51. Wurth, C.; Kessler, U.; Vogt, J.; Schulz, G.E.; Folkers, G.; Scapozza, L. The effect of substrate binding on the conformation and structural stability of Herpes Simplex virus type 1 thymidine kinase. *Protein Sci.* **2001**, *10*, 63. [[CrossRef](#)] [[PubMed](#)]
52. Khalil, R.M.; Abdelbary, G.A.; Basha, M.; Awad, G.E.A.; El-Hashemy, H.A. Design and evaluation of proniosomes as a carrier for ocular delivery of lomefloxacin HCl. *J. Liposome Res.* **2017**, *27*, 118–129. [[CrossRef](#)] [[PubMed](#)]
53. Wen, M.M.; Farid, R.M.; Kassem, A.A. Nano-proniosomes enhancing the transdermal delivery of mefenamic acid. *J. Liposome Res.* **2014**, *24*, 280–289. [[CrossRef](#)] [[PubMed](#)]
54. Shamma, R.N.; Basalious, E.B.; Shoukri, R.A. Development and optimization of a multiple-unit controlled release formulation of a freely water soluble drug for once-daily administration. *Int. J. Pharm.* **2011**, *405*, 102–112. [[CrossRef](#)] [[PubMed](#)]
55. Bayindir, Z.S.; Yuksel, N. Characterization of niosomes prepared with various nonionic surfactants for paclitaxel oral delivery. *J. Pharm. Sci.* **2010**, *99*, 2049–2060. [[CrossRef](#)]
56. Ismail, S.; Khattab, A. Optimization of proniosomal itraconazole formulation using Box Behken design to enhance oral bioavailability. *J. Drug Deliv. Sci. Technol.* **2018**, *45*, 142–150. [[CrossRef](#)]
57. Abdelbary, G.A.; Amin, M.M.; Zakaria, M.Y. Ocular ketoconazole-loaded proniosomal gels: Formulation, ex vivo corneal permeation and in vivo studies. *Drug Deliv.* **2017**, *24*, 309–319. [[CrossRef](#)]
58. Hathout, R.M.; Mansour, S.; Mortada, N.D.; Guinedi, A.S. Liposomes as an ocular delivery system for acetazolamide: In vitro and in vivo studies. *AAPS PharmSciTech* **2007**, *8*, E1–E12. [[CrossRef](#)]
59. Ramezani, V.; Honarvar, M.; Seyedabadi, M.; Karimollah, A.; Ranjbar, A.M.; Hashemi, M. Formulation and optimization of transfersome containing minoxidil and caffeine. *J. Drug Deliv. Sci. Technol.* **2018**, *44*, 129–135. [[CrossRef](#)]
60. Alsarra, I.A. Evaluation of proniosomes as an alternative strategy to optimize piroxicam transdermal delivery. *J. Microencapsul.* **2009**, *26*, 272–278. [[CrossRef](#)]
61. Mokhtar, M.; Sammour, O.A.; Hammad, M.A.; Megrab, N.A. Effect of some formulation parameters on flurbiprofen encapsulation and release rates of niosomes prepared from proniosomes. *Int. J. Pharm.* **2008**, *361*, 104–111. [[CrossRef](#)]
62. Marwa, A.; Omaima, S.; Hanaa, E.-G.; Mohammed, A.-S. Preparation and in-vitro evaluation of diclofenac sodium niosomal formulations. *Int. J. Pharm. Sci. Res.* **2013**, *4*, 1757–1765.
63. Pardakhty, A.; Varshosaz, J.; Rouholamini, A. In vitro study of polyoxyethylene alkyl ether niosomes for delivery of insulin. *Int. J. Pharm.* **2007**, *328*, 130–141. [[CrossRef](#)] [[PubMed](#)]
64. Aboelwafa, A.A.; El-Setouhy, D.A.; Elmeshad, A.N. Comparative study on the effects of some polyoxyethylene alkyl ether and sorbitan fatty acid ester surfactants on the performance of transdermal carvedilol proniosomal gel using experimental design. *AAPS PharmSciTech* **2010**, *11*, 1591–1602. [[CrossRef](#)] [[PubMed](#)]
65. Fang, J.Y.; Yu, S.Y.; Wu, P.C.; Huang, Y.B.; Tsai, Y.H. In vitro skin permeation of estradiol from various proniosome formulations. *Int. J. Pharm.* **2001**, *215*, 91–99. [[CrossRef](#)]
66. Zandi, K.; Ramedani, E.; Mohammadi, K.; Tajbakhsh, S.; Deilami, I.; Rastian, Z.; Fouladvand, M.; Yousefi, F.; Farshadpour, F. Evaluation of antiviral activities of curcumin derivatives against HSV-1 in Vero cell line. *Nat. Prod. Commun.* **2010**, *5*, 1935–1938. [[CrossRef](#)] [[PubMed](#)]

